

# EXPERIMENTS ON THE COMBUSTION BEHAVIOUR OF HYDROGEN-CARBON MONOXIDE-AIR MIXTURES

Friedrich, A.<sup>1</sup>, Necker, G.<sup>1</sup>, Vesper, A.<sup>1</sup>, Grune, J.<sup>1</sup>, Kuznetsov, M.<sup>2</sup> and Jordan, T.<sup>2</sup>

<sup>1</sup> Pro-Science GmbH, Parkstrasse 9, Ettlingen, 76275, Germany,  
<sup>2</sup> Karlsruhe Institute of Technology, Kaiserstrasse 12, Karlsruhe, 76131, Germany

## ABSTRACT

As a part of a German nuclear safety project on the combustion behavior of hydrogen-carbon monoxide-air mixtures small scale experiments were performed to determine the lower flammability limit and the laminar burning velocity of such mixtures. The experiments were performed in a spherical explosion bomb with a free volume of 8.2 liter. The experimental set-up is equipped with a central spark ignition and quartz glass windows for optical access. Further instrumentation included pressure and temperature sensors as well as high-speed shadow-videography. A wide concentration range for both fuel gases was investigated in numerous experiments from the lower flammability limits up to the stoichiometric composition of hydrogen, carbon monoxide and air (H<sub>2</sub>-CO-air) mixtures. The laminar burning velocities were determined from the initial pressure increase after the ignition and by using high-speed videos taken during the experiments.

## 1.0 INTRODUCTION

In severe nuclear reactor accidents with core meltdown high pressure and temperature loads to the safety containment can occur that might lead to local leakages of hydrogen and carbon monoxide formed due to the reaction of molten core and water or concrete. In such cases flammable H<sub>2</sub>-CO-air mixtures are generated in adjacent air-filled compartments [1]. Due to the high temperature and the low molecular weight (compared to air) of the released accident atmosphere these mixtures form stable stratified H<sub>2</sub>-CO-air layers. For the evaluation of the damage potential that is associated with such scenarios and as a basis for the development of mitigation measures the combustion behavior of such stratified H<sub>2</sub>-CO-air layers in semi-confined geometries has to be investigated.

The work reported here is part of a joint research project with the Technical University of Munich (TUM), but the scenario described is not restricted to severe reactor accidents, since similar hazardous situations are also conceivable e.g. in tunnel accidents, where a glowing fire might produce large amounts of CO and large quantities of H<sub>2</sub> are released from the damaged tank of a fuel-cell powered vehicle.

In safety research the pressure loads on the surrounding structures and safety equipment, which may be generated by an accidental flame initiated by a weak ignition, are of special interest. Since the pressure loads generated during the combustion of a premixed gas cloud are governed mainly by the flame velocity [2], the essential task is to evaluate a critical expansion ratio as a potential for flame acceleration to sonic speed (FA) and a detonation cell width as a scaling factor for detonation onset. As found in [2], the critical expansion ratio is a function of Zeldovich and Markstein numbers which are, in turn, also dependent on activation energy, initial temperature, reaction order and a number of thermodynamic properties. Such overall characteristics can be extracted from laminar flame velocities at different pressures, temperatures and mixture compositions. Then, a pre-requisite for the evaluation of flammability limits and laminar burning velocity for H<sub>2</sub>-CO-air mixtures is strongly required to evaluate or to predict all possible flame propagation regimes. Only few data on the combustion properties of H<sub>2</sub>-CO-air mixtures with different compositions are available. The main reason for this lack of data might be the acute toxicity of CO, whose Occupational Exposure Limit (OEL) is as low as 30 ppm, and so stringent safety precautions have to be fulfilled for its handling.

Most publications on the burning behavior of H<sub>2</sub>-CO-mixtures are related to SynGas, but only few articles address the burning behavior of H<sub>2</sub>-CO-air-mixtures with different compositions of the fuel gases. Burner-experiments on the laminar flame speed of H<sub>2</sub>-CO-air-mixtures were reported by Dong et al. in 2009 [3] for selected H<sub>2</sub>/CO ratios. In this paper also equations for the estimation of the laminar flame speed of pure H<sub>2</sub>-air- or CO-air-mixtures in different equivalence ratios are determined:

$$S_{H_2} = 0.08925 + 1.59163 \phi - 0.91917 \phi^2 + 0.52964 \phi^3 \quad (\phi = 0.7 - 2.1), \quad (1)$$

$$S_{CO} = 0.03276 + 0.18198 \phi - 0.04156 \phi^2 + 0.00791 \phi^3 \quad (\phi = 0.7 - 2.1), \quad (2)$$

where  $\phi$  is the equivalent ratio of the component in the mixture. In this work only rather fuel rich mixtures with fuel concentrations of more than 20 Vol% were investigated. But for the current work also lean mixtures are of special interest.

## 2.0 EXPERIMENTAL DETAILS

### 2.1 Test Facility

The experiments on the burning behavior of H<sub>2</sub>-CO-air mixtures were performed in a spherical stainless steel explosion bomb with an internal diameter of 25 cm ( $V = 8.2 \text{ dm}^3$ , Fig. 1 (left)), for further details see also [4] and [5]. The bomb has an optical access via two quartz windows and is equipped with ports for two fast dynamic pressure gauges and two NiCr/Ni thermocouples (type K). Mixtures inside the bomb are ignited using a high voltage (60 kV) high frequency (20 kHz) spark between two electrodes. Due to the design of the facility the electrodes meet in an angle of 90°, with the gap between them being positioned in the center of the spherical combustion chamber. A flow diagram of the test set-up is depicted in the right part of Fig. 1.

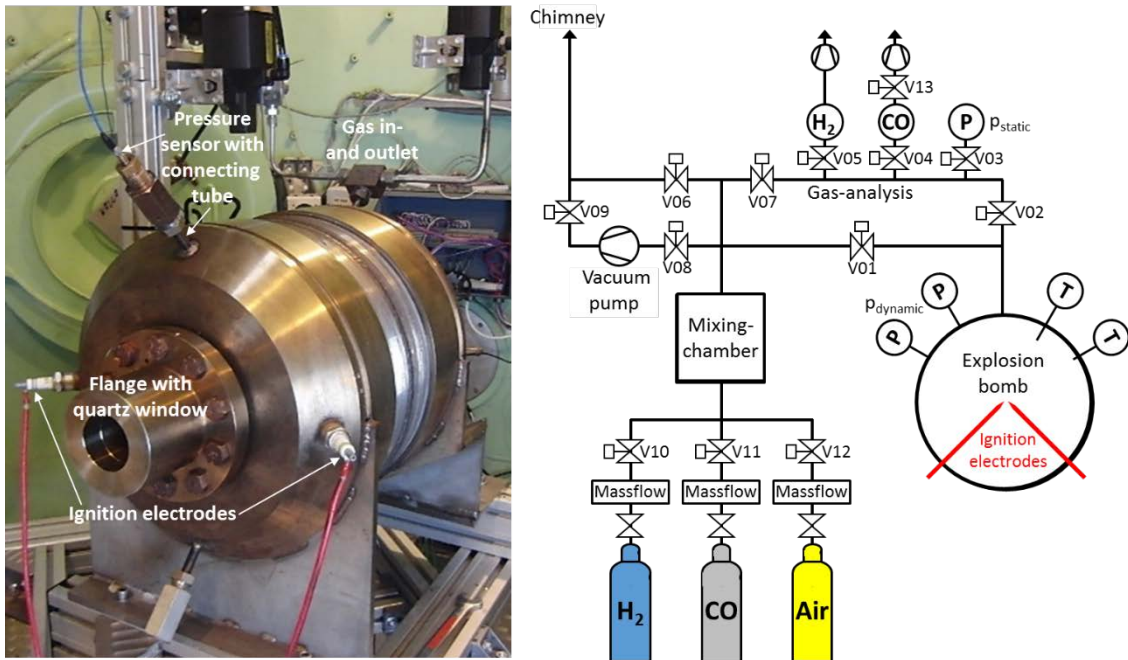


Fig. 1: Photo and flow diagram of the test facility.

The explosion bomb is filled with H<sub>2</sub>-CO-air mixtures using a gas mixing system that consists of three massflow controllers (Bronkhorst, Series F), a mixing chamber and a bypass line. The fuel gases are taken from gas bottles that are stored either in free field (H<sub>2</sub>) or in a cabinet with a CO-sensor (CO), while air is taken from the pressurized air grid available at KIT. The initial conditions of an experiment are monitored utilizing separate sensors for H<sub>2</sub> (Messkonzept, FTC 300, 0 – 100 Vol% H<sub>2</sub>)

and CO (Sensors Europe, S-AGM Plus, 0 – 35 Vol% CO) and a static pressure sensor (Leybold, DI 2001, 0 – 2000 mbar).

## 2.1 Test Procedure

Prior to any experiment the complete facility is evacuated to remaining pressures of less than 1 mbar. Then the mixture is generated in the mixing chamber using pre-calculated mass flows for the three components H<sub>2</sub>, CO and air to yield the desired mixture composition. When the pressure in the mixing chamber has reached approx. 1.2 bar its connection to the bypass line is opened, conducting the mixture flow through a chimney to the ambience, for safety reasons in a height of 6 m. At the same time the branch to the gas analysis is opened and the mixture composition in the mixing chamber is analysed by the sensors for H<sub>2</sub> and CO which are continuously extracting small mixture samples from the mixing chamber. When the desired mixture composition is reached in the mixing chamber the valves to bypass and gas-analysis are closed and the mixture is conducted into the evacuated bomb up to a slight overpressure, again approx. 1.2 bar absolute. Then the valve to the bomb is closed and the mixture is directed again through the bypass. During bypass flow the fuel-gas supplies are stopped and pipe system and mixing chamber are purged with air. Meanwhile the bomb is connected to the gas analysis and the exact H<sub>2</sub>- and CO-fractions in the mixture are determined. When, after several minutes of very slow depressurization via the gas sensors, a pressure of 1 bar (+/- 10 mbar absolute) is reached inside the bomb all valves are closed for the ignition. After the ignition and a certain delay time bomb and pipe system are evacuated again for the next experiment. With the method described it is possible to generate mixtures with an accuracy of +/- 4% of the desired concentration values for mixtures with fractions of > 5 Vol% for the fuel components. For fractions of less than 5 Vol% for one or more fuel components this method becomes less accurate, since the mass flow controllers have to provide very low mass flows against very low pressures in the initial phase of the filling procedure. In this case absolute deviations of the desired concentration are in the range of 0.4 Vol%. Anyway the exact mixture composition is measured with the sensors for H<sub>2</sub> and CO prior to the ignition and is also used in all further evaluations.

## 2.2 Ignition device

The H<sub>2</sub>-CO-air mixtures in the explosion bomb were ignited using an ignition device which produces a high voltage (60 kV) and high frequency (20 kHz) spark between two electrodes in the center of the explosion bomb. Usually an ignition duration of 100 ms was used, for experiments close to the flammability limit this duration was increased to 250 ms already in the first ignition attempt. When no ignition was observed a second ignition attempt with a duration of 0.5 s was performed with the same mixture, followed by a third attempt with 1 s and finally a manually controlled attempt with an ignition duration of > 2 s.

## 2.3 Pressure measurements

Accurate measurements of the pressure development inside the bomb during the experiment were used to evaluate the main combustion characteristics. To cover the different maximum pressure ranges of weak and reactive mixtures, as well as to allow thorough evaluation of the pressure rise rate in the initial phase of the combustion process, two fast dynamic pressure gauges with different measuring ranges (PCB, Type 113B36 (0 – 3.5 bar, P1) and Type 113B26 (0 – 35 bar, P2)) were connected via short tubes to the explosion bomb (see Fig. 1, left). Typical pressure records of these sensors for a rather reactive mixture are plotted in the left part of Fig. 2. The course of sensor P1 ends already at a pressure level close to 0.7 bar, since only the initial range of the combustion process, up to a pressure value of approx. 2% of the maximum pressure, will be used in the later evaluation. Nevertheless, the values measured by P1 in the initial phase of the experiment show good agreement with the signal of P2, which was recorded up to the maximum overpressure values of approx. 6.5 bar ( $t \approx 0,025$  s) and 11 bar ( $t \approx 0,039$  s). The second maximum occurs as a narrow peak almost 15 ms after the initial pressure increase is over and is due to the tiny tubes that are used to connect the pressure sensors with the combustion chamber. When the mixture is ignited the flame expands spherically until it reaches

the bomb wall where it quenches and where heat losses cause a slow decrease of the measured pressure. Then, due to the combustion of the unburnt and pre-compressed mixture in the tiny tubes to the pressure gauges, a short term pressure impulse is generated, which is typical for the facility. For the evaluation of the experiment only the first maximum overpressure of the combustion in the spherical chamber is of interest.

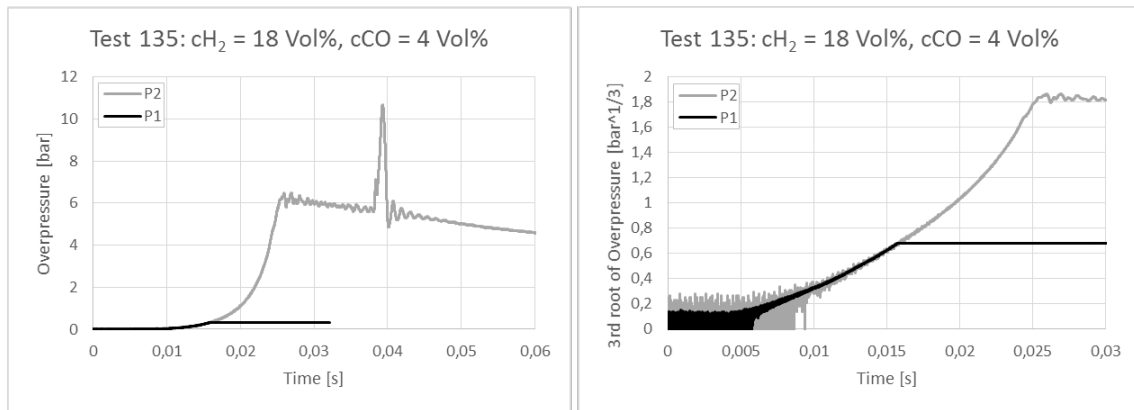


Fig. 2: Typical records of the two dynamic pressure sensors P1 and P2 for an experiment with a reactive mixture (left), and linearization of the pressure courses (right).

A spherical flame front propagating in a spherical vessel produces a pressure record which follows a cubic function [6]. Thus the third root of the pressure history shows an almost linear time dependence (Fig. 2, right), indicating a quasi-constant visible flame speed from the ignition position to the wall. More complex is the interpretation of the flame propagation inside the spherical chamber for mixtures close to the flammability limit. In the pressure records of such experiments low flame velocities lead to an increasing influence of buoyancy that might hinder the flame from burning in downward direction, or other effects like quenching of the flame due to high heat losses might occur. So the pressure history does not follow a cubic law for a significant time duration and thus an evaluation of the visible flame velocity using the pressure records is not possible. In the current work experiments were omitted, when the regression coefficient of the final linearization was  $R^2 < 0.99$ . In this case the optical observation inside the spherical chamber can be useful for data interpretation.

### 2.3 Flame visualization

For the investigation of the early part of the combustion process, especially in lean mixtures, an additional high speed shadowgraphy set-up using the optical access via the two quartz glass windows of the bomb (visible window size  $d = 50$  mm) was installed for the second half of the test series. Due to the spatial restrictions inside the safety vessel no ideal set-up was possible, but nevertheless good quality high speed movies could be recorded. In the tests the frame rate of the high speed camera (Photron FASTCAM-SA1.1) was varied from 1.000 – 10.000 frames/s.

Fig. 3 shows images taken from high-speed movies (10.000 fps) of three experiments with 12 Vol% fuel. In the top row pure hydrogen was used as fuel ( $cH_2 = 12$  Vol%) while in the center row equal fractions of H<sub>2</sub> and CO were used ( $cH_2 = cCO = 6$  Vol%). In the experiment shown in bottom row of Fig. 3 a mixture containing 2 Vol% H<sub>2</sub> and 10 Vol% CO was ignited.

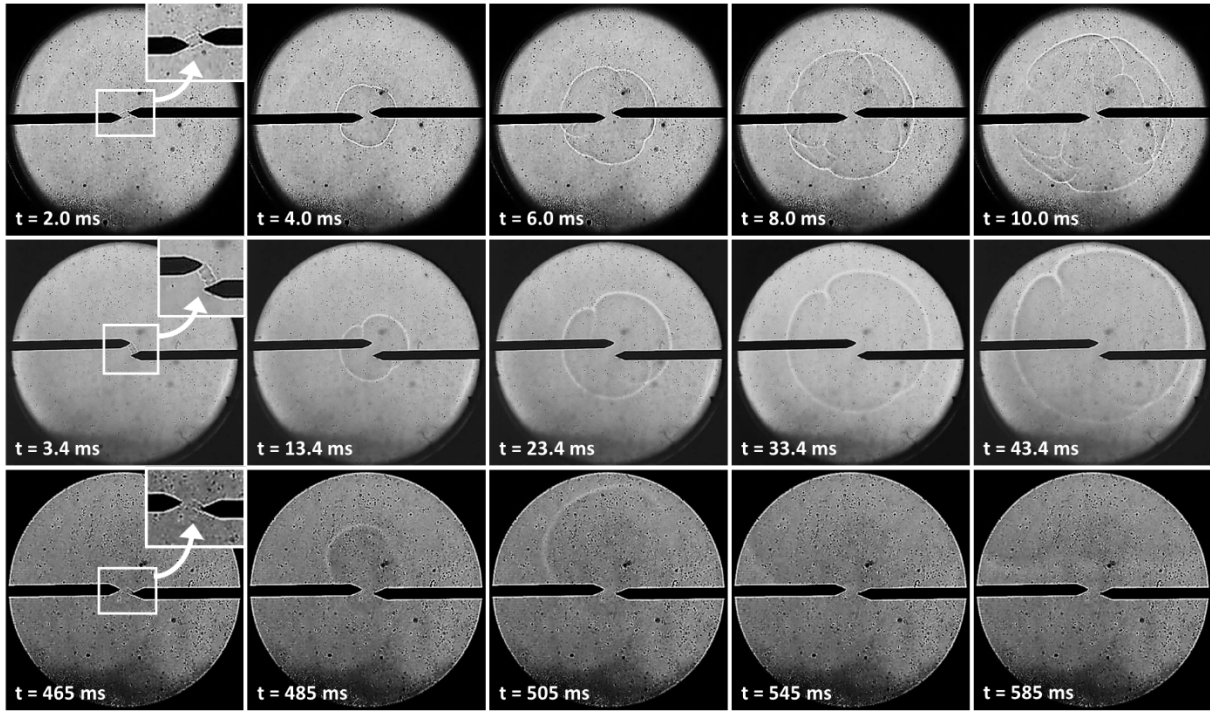


Fig. 3: High speed movies (10.000 fps) of the initial combustion processes in mixtures with 12 Vol% of fuel. Top row: 12 Vol% H<sub>2</sub> in air, center row: cH<sub>2</sub> = cCO = 6 Vol% in air, bottom row: 2 Vol% H<sub>2</sub> and 10 Vol% CO in air.

In the pure H<sub>2</sub>-air mixture (cH<sub>2</sub> = 12 Vol%) the ignition occurs almost immediately and the flame expands almost spherically in all directions from the ignition point (top row in Fig. 3). The visible surface of the flame is wrinkled and also complex structures can be recognized inside the growing sphere, which are due to the influence of flame stretch and instabilities. In this case the borderline of the sphere is captured very sharp in the HS-movie and its diameter can be measured accurately. So in principle, using the increase of the radius and the frame rate of the camera; a visible flame velocity can be determined for each time span in between two images. But due to the limited spatial resolution of the camera, compared to its large time-resolution, the difference in the radii (and correspondingly the time span) in between the images has to be chosen large enough for an accurate determination of the velocity. For a mixture where half of the H<sub>2</sub> content is replaced by CO (cH<sub>2</sub> = cCO = 6 Vol%, center row in Fig. 3) the ignition occurs slightly delayed and the propagation of the rather smooth spherical flame front is significantly slower and shows almost no structures inside the sphere. Furthermore already slight buoyancy effects can be observed, since the center of the sphere, representing the flame front in the HS-images, moves slightly in upward direction. Although the borderline of the sphere is slightly fuzzy an evaluation of the diameter of the growing sphere is still possible and thus again visible flame velocities can be determined. But due to the difficulties in the diameter measurements these velocities have a higher inaccuracy. In a mixture that contains only 2 Vol% H<sub>2</sub> but 10 Vol% CO a significant delay of the ignition is observed and the developing slow flame is strongly distorted due to buoyancy effects. In the first part of this experiment almost no flame is detected below the ignition position and after the end of the ignition the flame lifts up and leaves the electrodes in upward direction. But approximately 420 ms later, at t ≈ 910 ms, the flame enters again the area covered by the video observation passing slowly in downward direction. In the initial phase of the HS-movie the flame front is hardly visible and shows no regular shape in its diffuse borderline. Thus a reliable determination of a visible burning velocity is not possible in such cases.

The pressure records of the experiment shown in the bottom HS-video sequence in Fig. 3 are plotted in the left part of Fig. 4. The graph shows, that the pressure record has several inflection points on its way to the first maximum, after which the pressure slowly decreases. Taking into account, that the

maximum overpressure recorded amounts to only 0.67 bar, compared to the calculated value for a complete adiabatic isochoric combustion pressure of the mixture of  $p_{AICC} = 4.15$  bar [7], it is obvious that no complete combustion of the mixture had occurred. Thus the pressure method should also not be applied to the data of this experiment to determine the burning velocity of the mixture.

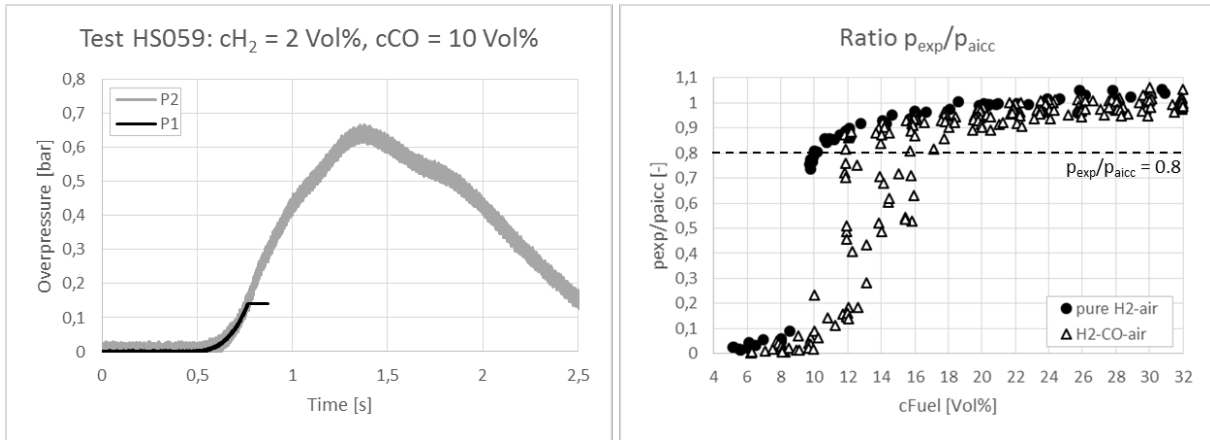


Fig. 4: Pressure records for the experiment of the bottom image series of Fig. 3 (left), and pressure ratios  $p_{exp}/p_{aicc}$  of selected experimental series' (right).

As the above examples demonstrate, it was not possible to determine laminar burning velocities for all experiments in which an ignition was observed. During evaluation it was decided not to rely on data of experiments where maximum overpressures of less than 80% of the calculated complete adiabatic isochoric combustion pressure were reached. The right graph in Fig. 4 summarizes the ratio  $p_{exp}/p_{aicc}$  for all experiments and shows that especially experiments with rather low fuel contents had to be omitted. So for pure H<sub>2</sub>-air mixtures a sharp cut occurs at a H<sub>2</sub>-concentration of approx. 10 Vol%, while the cut occurs at fuel concentrations between 12 and 16 Vol% for experiments with H<sub>2</sub>-CO-air-mixtures. Above fuel concentrations of 16 Vol% an almost complete combustion was observed in all experiments H<sub>2</sub>-CO-air-mixtures.

### 3.0 RESULTS AND DISCUSSION

#### 3.1 Test matrix

In the test series almost the complete lean concentration range for mixtures up to 30 Vol% fuel gas (stoichiometric concentration for both fuel gases in air is 29.6 Vol%) was investigated in steps of 2 Vol% for both fuel gases (see Fig. 5). Some of the experiments were repeated to check the reproducibility of the results, others had to be repeated since no ignition was observed in the first ignition attempt. Most of the experiments were performed with an ignition duration of 100 ms, but when approaching the flammability limit this time was extended to 250 ms already for the first ignition attempt. In case no ignition was observed in the first attempt, further attempts were made where the ignition duration was increased stepwise. So in total almost 400 ignition attempts were made to investigate the combustion behavior of H<sub>2</sub>-CO-mixtures, but in roughly 120 of these experiments no ignition was observed ("x" in Fig. 5).

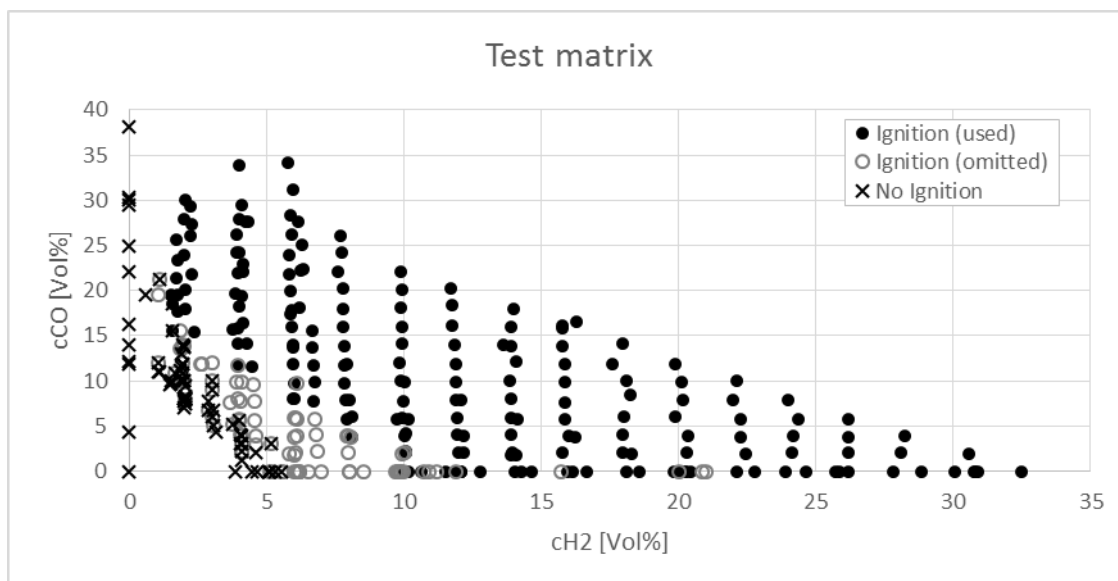
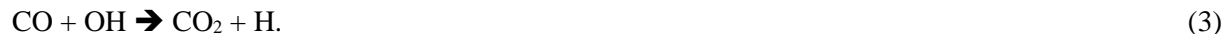


Fig. 5: Test matrix: Closed circles represent experiments with ignition that were used for the evaluation while open circles stand for experiments with ignition that were omitted. Crosses indicate that no ignition was observed in the experiment.

Although several attempts were made, it was not possible to ignite pure CO-air mixtures during the complete series. The reason is that the reaction of a dry CO-O<sub>2</sub> mixtures is very slow even at high temperatures [8], but the overall reactivity is greatly accelerated in the presence of trace amounts of moisture or H<sub>2</sub>, since the dominant path for CO oxidation leading to the formation of CO<sub>2</sub> is the exothermic reaction



In the bomb experiments described here dry air was used to generate the mixture and thus no ignition of CO-air mixtures without H<sub>2</sub> was possible due to the lack of OH-radicals. Attempts to overcome this difficulty by using ambient air for the mixture preparation, or by not performing a complete evacuation of the bomb after an experiment with high H<sub>2</sub>-content (producing large amounts of humidity inside the bomb) at the end of the campaign did not succeed. The lack of humidity might also be the reason for the observed ignition behavior of some very lean mixtures that could not be ignited in several attempts, but then ignited immediately, since small amounts of humidity were produced close to the ignition source in the previous ignition attempts.

### 3.2 Lower flammability limits (LFLs) of H<sub>2</sub>-CO-air mixtures

The main aim of the work reported here was to determine the combustion properties of H<sub>2</sub>-CO-air mixtures for conditions similar to the conditions of the planned large scale experiments in a combustion channel. So in the complete test series only one standard ignition device (see above) was used under ambient temperature and pressure conditions.

In the frame of the investigations a mixture was labelled inflammable when it was not possible to ignite it in 4 (in very few cases 5) ignition attempts with increasing ignition duration (see 2.2). The ignition of the mixture was determined using the pressure signals and, if available, the HS-video records of the experiments. For comparison one experiment was performed without fuel to determine the pressure generated by the thermal energy of the ignition source itself. In this experiment no pressure increase could be determined at all, and so a pressure increase of 1% of the initial pressure was found to be sufficient to prove an ignition of the mixture. Most mixtures with rather high fuel concentrations ignited already in the first attempt, but with decreasing fuel, and especially H<sub>2</sub>-content, it became more and more difficult to ignite the test mixtures. The experiments close to the

flammability limit are summarized in the left graph of Fig. 6, where grey dots show that the mixture was ignited, while decreasing size indicates that several attempts (number of attempts in brackets) were needed. Black crosses symbolize that no ignition of the mixture was observed.

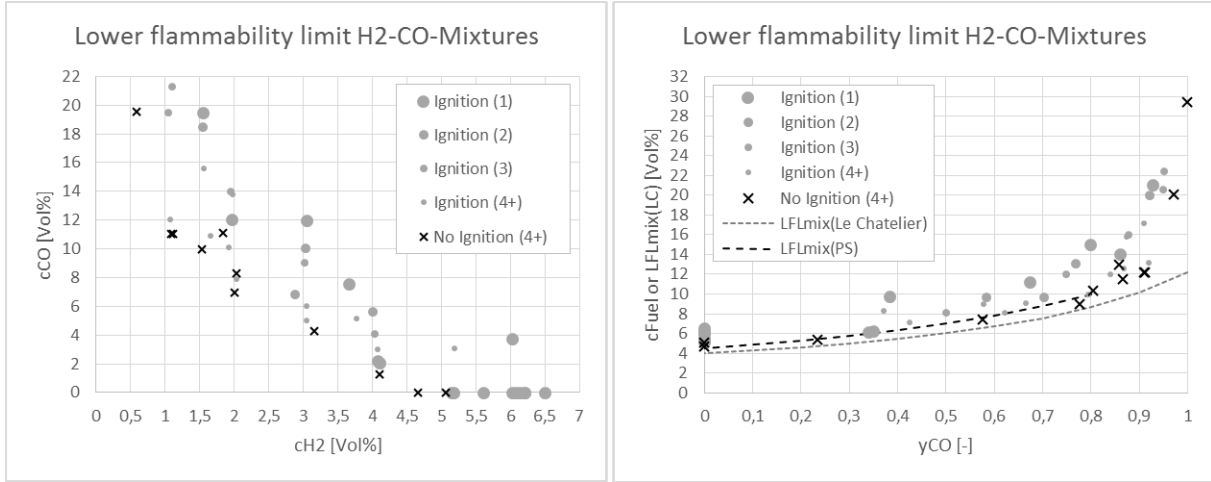


Fig. 6: Test matrix of experiments close to the lower flammability limit of H<sub>2</sub>-CO-air mixtures (left) and comparison of results with calculated flammability limits according to Le Chatelier's rule and flammability limits taken from literature (right). Grey dots with different sizes indicate that several attempts (number of attempts in brackets) were needed to ignite the mixture, black crosses symbolize that no ignition was observed.

The left graph of Fig. 6 shows that in the facility used it was not possible to ignite H<sub>2</sub>-air mixtures with H<sub>2</sub>-concentrations of less than 5.2 Vol% H<sub>2</sub>, although the lower flammability limit for such mixtures is given with 4.0 Vol% in literature [9]. As mentioned above, it was also not possible to ignite pure CO-air mixtures due to the lack of humidity in the test mixtures. The mixture with the lowest H<sub>2</sub>- and fuel concentration that could be ignited had a H<sub>2</sub>-concentration of 1.1 Vol% and a CO-concentration of 12.1 Vol%. This CO-concentration lies in the range of the LFL of pure CO-air mixtures (12.2 Vol% CO in air) given in literature [10]. So with the ignition source and the facility used it was not possible to approach the absolute LFL of the binary mixtures. To compare the results of the experiments with literature data Le Chatelier's mixing rule for lower flammable limits of mixtures was used [11].

$$LFL_{mix(LC)} = \frac{1}{\sum_{i=1}^N \frac{y_i}{LFL_i}}, \quad (4)$$

where  $LFL_{mix}$  and  $LFL_i$  are the lower flammability limits of mixture and component  $i$  [Vol%],  $N$  is the number of flammable components [-] and  $y_i$  is the molar fraction of component  $i$  [-]. The result of this approximation is plotted as dotted line together with the experimental results in the right graph of Fig. 6. For low molar fractions of CO the difference between calculated and experimental limits is rather small and almost constant, but for molar fractions of CO larger than 0.8 the deviation becomes larger, most likely due to the influence of lacking humidity. Nevertheless it is possible to describe the LFL-behavior of the current facility for mixtures with molar fractions of CO of less than 0.8 by extending Le Chatelier's mixing rule in the following way:

$$LFL_{mix(PS)} = LFL_{mix(LC)} + y_{CO} + 0.5, \quad (5)$$

where  $y_{CO}$  is the molar fraction of CO in the test mixture. This function is plotted as black dashed line in the right graph of Fig. 6.

### 3.3 Laminar burning velocities of H<sub>2</sub>-CO-air mixtures

For the determination of the laminar flame speed of a mixture mostly burner set-ups or bomb facilities are used. At KIT a bomb method is used, where mixtures are ignited by a spark in the center of a spherical cavity. The method developed by Andrews and Bradley [12] was already used slightly modified for the determination of burning velocities on the basis of the experimental pressure records in previous work [5]. The governing formulas are repeated below, a more detailed description may be found there.

To evaluate the laminar burning velocity the dependence which takes into account the adiabatic change of pressure and temperature of the unburned material was used [13]:

$$S_L = \frac{S_S}{\sigma} \left( 1 + \frac{1}{\gamma_b} \frac{B_2 r_b^3}{(S_S^3 P_0 + B_2 r_b^3)} \right), \quad (6)$$

Here  $B_2$  is the polynomial coefficient of the correlation of the experimental pressure–time history in the form

$$p(t) = p_0 + B_2 \cdot t^3, \quad (7)$$

where  $p_0$  is the ambient pressure [bar],  $r_b$  is the burned gas radius [m],  $\sigma = \rho_u/\rho_b$  is the expansion rate of burned mixture [-],  $\gamma_b, \gamma_u$  are specific heat ratios for the burned and unburned gas and  $S_S$  is the visual flame velocity given by:

$$S_S = \left( \frac{B_2}{P_0} \left( \frac{\gamma_b R^3 + \frac{\gamma_u}{\sigma} r_b^3 - \gamma_b r_b^3}{(1 - \frac{1}{\sigma}) \gamma_b \gamma_u} \right) \right), \quad (8)$$

where  $R$  is the internal radius of the explosion chamber [m].

The evaluation procedure shall be explained using the two graphs of Fig. 7 for an experiment with a H<sub>2</sub>-content of 25.7 Vol%.

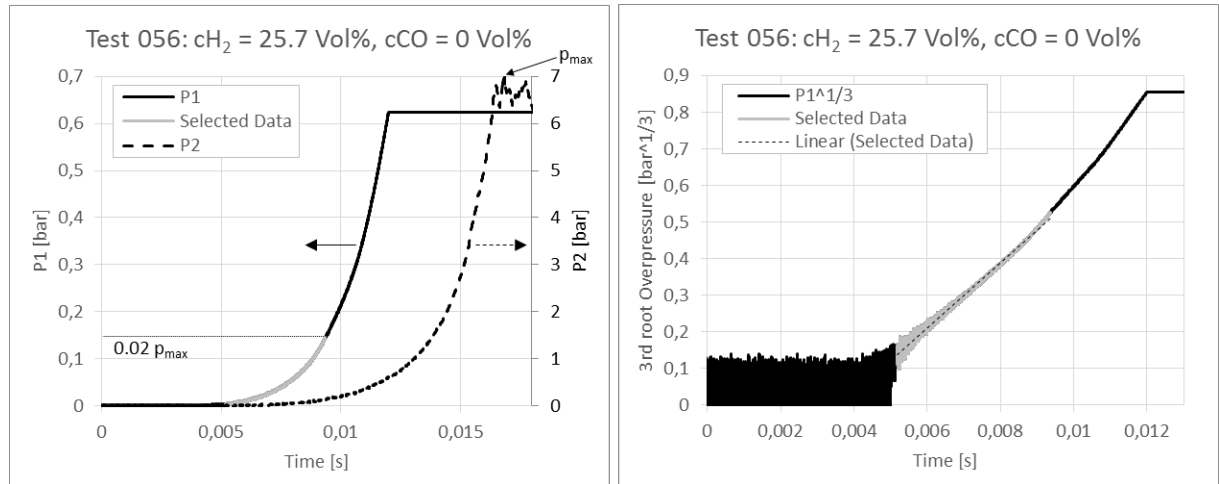


Fig. 7: Left: Pressure histories of both pressure sensors used in the experiment (solid and dashed black lines) and selected pressure range for the evaluation (grey). Right: Linearization of the selected range.

The two pressure signals recorded during the experiment are shown in the left graph of Fig. 7 as solid and dashed black lines. The dashed curve of sensor P2 was used to determine the maximum pressure recorded during the test ( $p_{\max} \approx 7$  bar) while the grey highlighted part of the record of the more sensitive sensor P1 (solid black line) was used to determine the burning velocity. A pressure value of 2% of the maximum pressure value was chosen as upper margin for the highlighted area to minimize influence of the increasing bomb pressure on the burning velocity. The right graph of Fig. 7 illustrates

that this initial part of the record can be linearly approximated as a cubic root of the pressure dependence vs. time Eq. (6), where  $B_2$  is the coefficient used to calculate the flame velocity according to the Eq. (6)–(8). In the example a visual flame velocity of  $S_S = 10.34$  m/s and a normal laminar flame velocity of  $S_L = 1.51$  m/s with an expansion ratio of  $\sigma = 6.938$  are determined.

To allow a comparison of the current experimental data with literature also a series of experiments with pure hydrogen-air mixtures was performed. Another comparison with literature data was possible for stoichiometric fuel-air mixtures with various  $H_2/CO$  ratios that were reported by Dong et al. [3]. Both comparisons are depicted in Fig. 8.

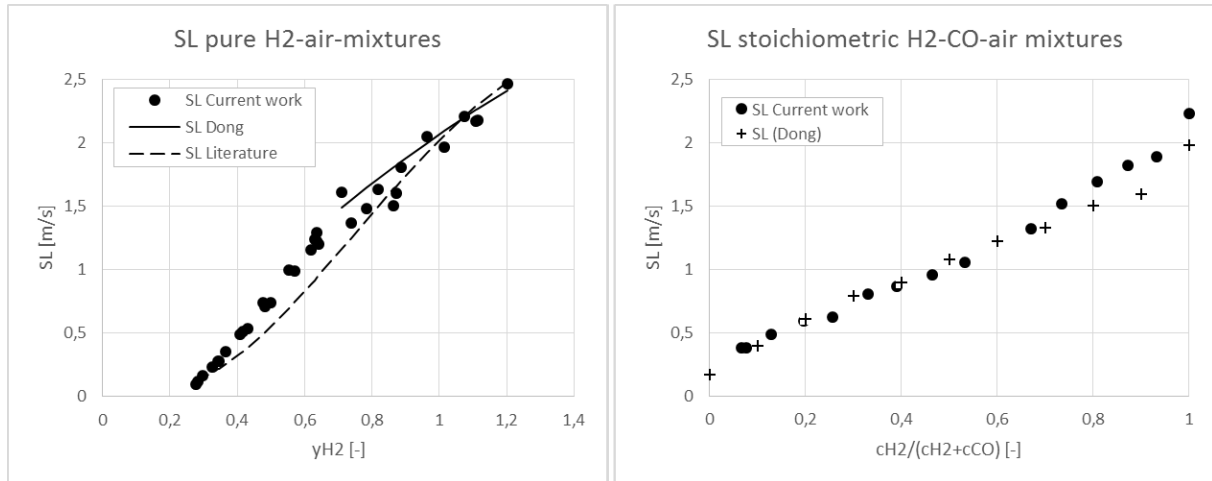


Fig. 8: Left: Comparison of  $S_L$  values for pure  $H_2$ -air-mixtures (without CO) of current work with literature data. Right: Comparison of  $S_L$  values for stoichiometric fuel-air-mixtures with various  $H_2/CO$  ratios of current work with values extracted from graph in [3].

The left graph in Fig. 8 shows that the laminar flame speeds determined using the pressure method described above show good agreement with the formula published by Dong et al. [3]. But according to the authors the formula is only valid for equivalent ratios from 0.7 to 2.1, which only covers the fuel rich part of the current work. Therefore, additionally, the current values were compared with the data provided in [14] (dashed line). Larger deviations of the current value can be found in the equivalent ratio region from 0.4 to 0.7, where influences of flame stretching and instabilities are important. But the velocities of the current work were determined mainly using the pressure method, and so no compensation of these effects was possible and thus the higher velocities of the current work seem reasonable. The comparison of laminar flame speeds for stoichiometric ( $c_{Fuel} \approx 30$  Vol%)  $H_2$ -CO-air mixtures with data from [3] is shown in the right graph of Fig. 8. Most velocities determined in the current work show good agreement with the literature data, larger deviations are solely found for high  $H_2$ -fractions of more than 70% in the fuel.

After the method was proven against available literature data the laminar flame speeds determined in the current work were plotted over the equivalent ratio for CO in different experimental series of equal fuel concentrations. For clearness Fig. 9 only shows selected series' which cover the main behavior observed in the tests.

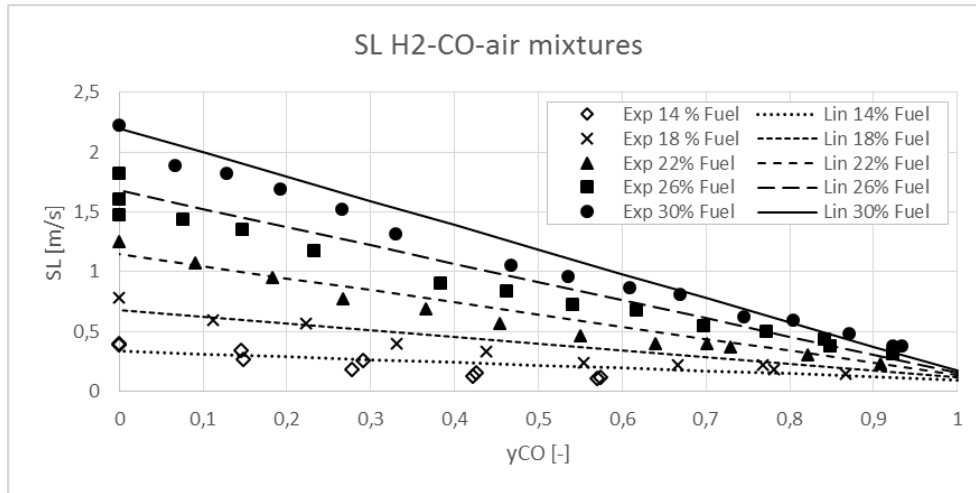


Fig. 9: Results of selected experimental series' on the laminar burning velocities of H<sub>2</sub>-CO-air-mixtures with the same fuel content but different H<sub>2</sub>/CO-ratios.

As the curves in Fig. 9 show, the laminar flame velocities of the mixtures decrease with increasing CO-fraction in the fuel. Starting from the values for pure H<sub>2</sub>-air-mixtures at  $y_{CO} = 0$  they decrease almost linearly to the value for pure CO-air-mixtures at  $y_{CO} = 1$ . To approach this behavior a simple correlation in the following form can be assumed

$$SL_{mix} = y_{H_2} \cdot SL_{H_2} + y_{CO} \cdot SL_{CO}, \quad (9)$$

where  $SL_{mix}$ ,  $SL_{H_2}$  and  $SL_{CO}$  are the laminar flame velocities of the mixture and the components H<sub>2</sub> and CO [m/s] and  $y_{H_2}$  and  $y_{CO}$  are the molar fractions of the fuel components H<sub>2</sub> and CO in the mixture [-].

Since only few values for  $SL_{CO}$  were available, Eq. (2) was used to calculate the values for pure CO-air mixtures. But as mentioned above this formula was derived for CO-concentrations above 22 Vol%. Nevertheless the formula was extrapolated down to concentrations of 12 Vol% CO for this evaluation, which led to increasing deviations of the linear approximation from the experimental values in CO rich mixtures, especially for fuel concentrations lower than 16 Vol%. For the lowest fuel concentration plotted in the graph (14 Vol%), for instance, an assumed  $SL$ -value of 0 m/s would lead to a much better result than the utilisation of the calculated value of approx. 0,1 m/s, which seems to be far too high. More accurate values for the laminar burning velocity of pure CO-air mixtures would therefore help to further increase the accuracy of the proposed approximation.

#### 4.0 CONCLUSIONS

Well known experimental data on the combustion behavior of H<sub>2</sub>-CO-air mixtures in various compositions were significantly extended in order to provide a basis for accident analyses of scenarios where H<sub>2</sub> and CO are generated.

The experimental investigation on the combustion behavior of H<sub>2</sub>-CO-air-mixtures up to the stoichiometric composition (approx. 30 Vol% fuel in air) was performed using a bomb facility with optical access at KIT. In numerous experiments flammability limits and laminar burning velocities were investigated using pressure measurements and a high-speed shadowgraphy system. An analysis of the experimental data showed that Le Chatelier's mixing rule for lower flammable limits of mixtures can be used as a conservative measure to determine the LFL of H<sub>2</sub>-CO-air mixtures. For a wide range of fuel concentrations with various H<sub>2</sub>/CO ratios laminar burning velocities were determined. To check the results the values for pure H<sub>2</sub>-air-mixtures and stoichiometric H<sub>2</sub>-CO-air-mixtures were compared successfully with literature data, if available. As a result an easy-to-use

correlation was proposed for the estimation of laminar burning velocities for different mixture compositions using the laminar burning velocities of the two fuel components of the mixture.

The current work shows that CO-fractions in H<sub>2</sub>-air mixtures can neither be neglected nor treated as H<sub>2</sub>, since both, addition of CO and replacement of H<sub>2</sub> by CO in H<sub>2</sub>-air mixtures have an influence on the combustion behavior of the mixture.

## 5.0 ACKNOWLEDGEMENTS

The authors are very grateful to the German Federal Ministry for Economic Affairs and Energy (BMWi) for funding (Project No. 1501545B), and also to the partners from the Chair of Thermodynamics at the Technical University of Munich (TUM) for fruitful discussions and support in the current work.

## 6.0 REFERENCES

1. Hessheimer, M.F., Dameron, R.A., Containment Integrity Research at Sandia National Laboratories – An Overview, NUREG/CR-6906, SAND2006-2274P (July 2006)
2. Dorofeev S.B., Kuznetsov M.S., Alekseev V.I., Efimenko A.A., Breitung W. Evaluation of limits for effective flame acceleration in hydrogen mixtures. *Journal of Loss Prevention in the Process Industries*, 2001, Vol 14/6, pp. 583-589
3. Dong C., Zhou Q., Zhao Q., Zhang Y., Xu T., Hui S., Experimental study on the laminar flame speed of hydrogen/carbon monoxide/air mixtures, *Fuel* 88 (2009) 1858–1863
4. Grune J., Breitung W., Kuznetsov M., Yanez J., Jang W., Shim W., Flammability limits and burning characteristics of CO-H<sub>2</sub>-H<sub>2</sub>O-CO<sub>2</sub>-N<sub>2</sub> mixtures at elevated temperatures, *International Journal of Hydrogen Energy* (2015), Volume 40, Issue 31, 17 August 2015, pp. 9838-9846
5. Kuznetsov M., Redlinger R., Breitung W., Grune J., Friedrich A., Ichikawa N., Laminar burning velocities of hydrogen-oxygen-steam mixtures at elevated temperatures and pressures, *Proceedings of the Combustion Institute*, Volume 33, Issue 1, 2011, pp. 895-903
6. Dahoe AE, Zevenbergen JF, Lemkowitz SM, Scarlett B. Dust explosions in spherical vessels: the role of flame thickness in the validity of the ‘tube-root law’. *J Loss Prev Process Ind* 1996;9(I):33e44.
7. Goodwin DG. *Cantera user's guide*. Pasadena, CA: California Institute of Technology; November, 2001.
8. Sung C.-J., Law C.K., *Fundamental Combustion Properties of H<sub>2</sub>/CO Mixtures: Ignition and Flame Propagation at Elevated Pressures*, *Combustion Science and Technology*, 180:6, 1097-1116
9. R.K. Kumar, Flammability limits of hydrogen–oxygen–diluent mixtures, *J. Fire Sci.* 3 (1985) 235–262.
10. . I.A. Zlochower and G.M. Green, The Limiting Oxygen Concentration and Flammability Limits of Gases and Gas Mixtures, *Journal of Loss Prevention in the Process Industries*, 2009, Vol. 22, No. 4, pp. 499–505.
11. Le Chatelier, H., Estimation of Firedamp by Flammability Limits, *Ann. Mines*, Vol. 19, ser. 8, pp.388-395, (1891).
12. Andrews, G.E. and Bradley, D. (1973) Burning velocity of methane-air mixtures. *Combust. Flame*, 18, 133–153
13. A.I. Gavrikov, A.V. Bezmelnitsyn, A.L. Lelyakin, S.B. Dorofeev. In: *Proc. of 18th Int. Colloquium on Dynamics of Explosions and Reactive Systems*, 2001, ISBN# 0-9711740-0-8, pp. 139.1–139.5.
14. Kuznetsov, M., Kobelt, S., Grune, J., Jordan, T., Flammability limits and laminar flame speed of hydrogen–air mixtures at sub-atmospheric pressures, *International Journal of Hydrogen Energy*, 37, 2012, pp. 17580-17588